The Gaia Initial QSO Catalog

Alexandre H. Andrei (Observatório Nacional/MCT, and associated researcher to CAR/University of Hertfordshire, SYRTE/Observatoire de Paris and Observatório do Valongo/UFRJ), Sonia Anton (Centro de Investigação em Ciências Geo-Espaciais/FCUP and SIM), François Taris (SYRTE/Observatoire de Paris), Geraldine Bourda (Observatoire de Bordeaux), Jean Souchay (SYRTE/Observatoire de Paris), Sébastien Bouquillon (SYRTE/Observatoire de Paris), Christophe Barache (SYRTE/Observatoire de Paris), J.J. Pereira Osório (Centro de Investigação em Ciências Geo-Espaciais/FCUP), Patrick Charlot (Observatoire de Bordeaux), Roberto Vieira Martins (Observatório Nacional/MCT), Sébastien Lambert (SYRTE/Observatoire de Paris), Júlio I. Bueno de Camargo (Observatório Nacional/MCT), Dario N. da Silva Neto (UEZO), Marcelo Assafin (Observatório do Valongo/UFRJ), Jean-François Le Campion (Observatoire de Bordeaux)

GWP-S-335-13000

Gaia DPAC Data Processing & Analysis Consortium

gaia

Purpose of the GIQC

● The manifold Gaia scientific output relies on precise astrometry accurate to sub-uas standards.

● This depends on building a fundamental reference frame formed by pointlike, position stable, and allsky homogeneous grid points.

☺ In one word, quasars.

☻ The Gaia CU3 Initial Quasar Catalogue Working Package was established to beforehand produce one such list, although ultimately the satellite multiband photometry aided by astrometric monitoring has the potential to pick up a clean sample of quasars.

Purpose of the GIQC – On board classification

♦ Also for QSOs the Gaia survey will be unique.

♦ Therefore a Gaia self-sufficient QSO recognition scheme is required.

♠ The method of choice is photometric identification

♠ Using of the prism dispersion Blue and Red Photometers images

♠ Led initially by J.F. Claeskens (Univ. of Liège, Belgium)

♠ Then continued by C. Bailer Jones (MPIA, Germany)

♥ Template set from synthetic library covering the full wavelength range sampled by Gaia (λ 2400 – 10500A), modeling the continuous slope and the lines intensity.

♥ To select a small clean sample of QSOs free of stellar contaminants

♥ To identify the majority of the QSOs in a not so clean sample

♣ Main contaminants: very red (M stars), or highly reddened stars and peculiar white dwarfs (and stars in general over the 2<z<3 interval)

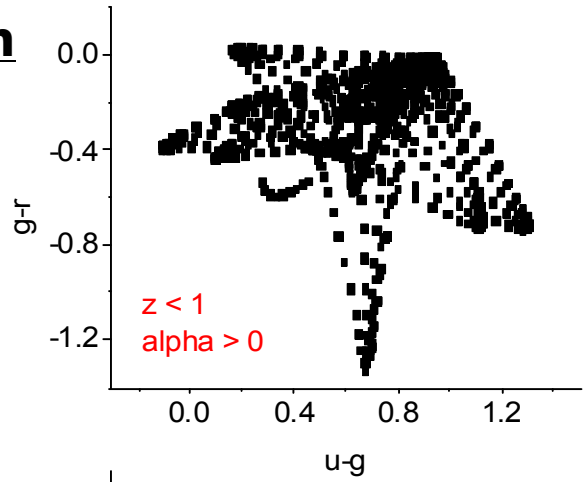

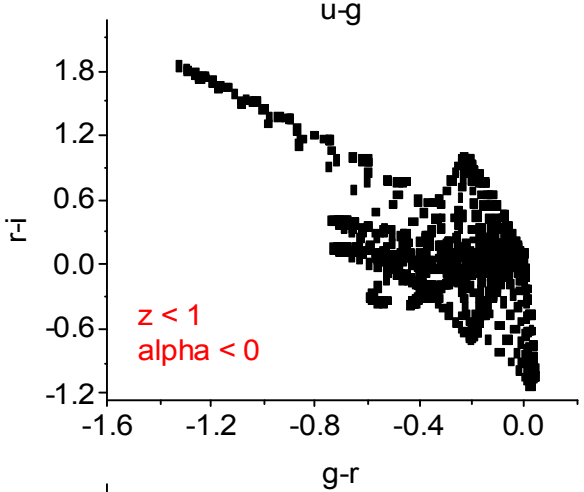

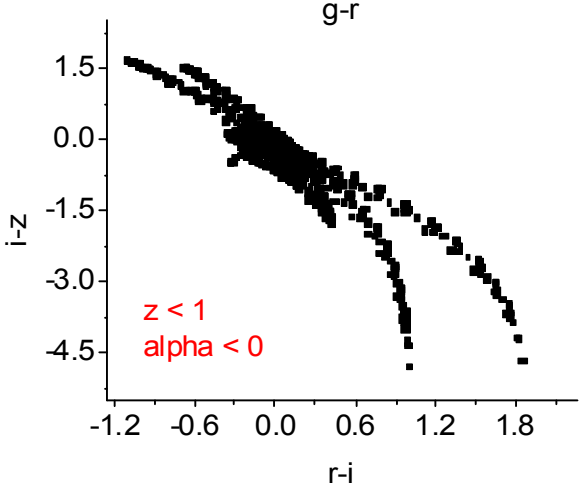

Purpose of the GIQC – On board classification

☺ The objects sample completeness is 99% with a contamination of 0.7%.
Including parallax and proper motion in the classifier barely changes the results.

● Morphology (host galaxy signature) and variability locus might be also included

♣ Not accounting for class priors in the target population leads to misclassifications and poor predictions for sample completeness and contamination.

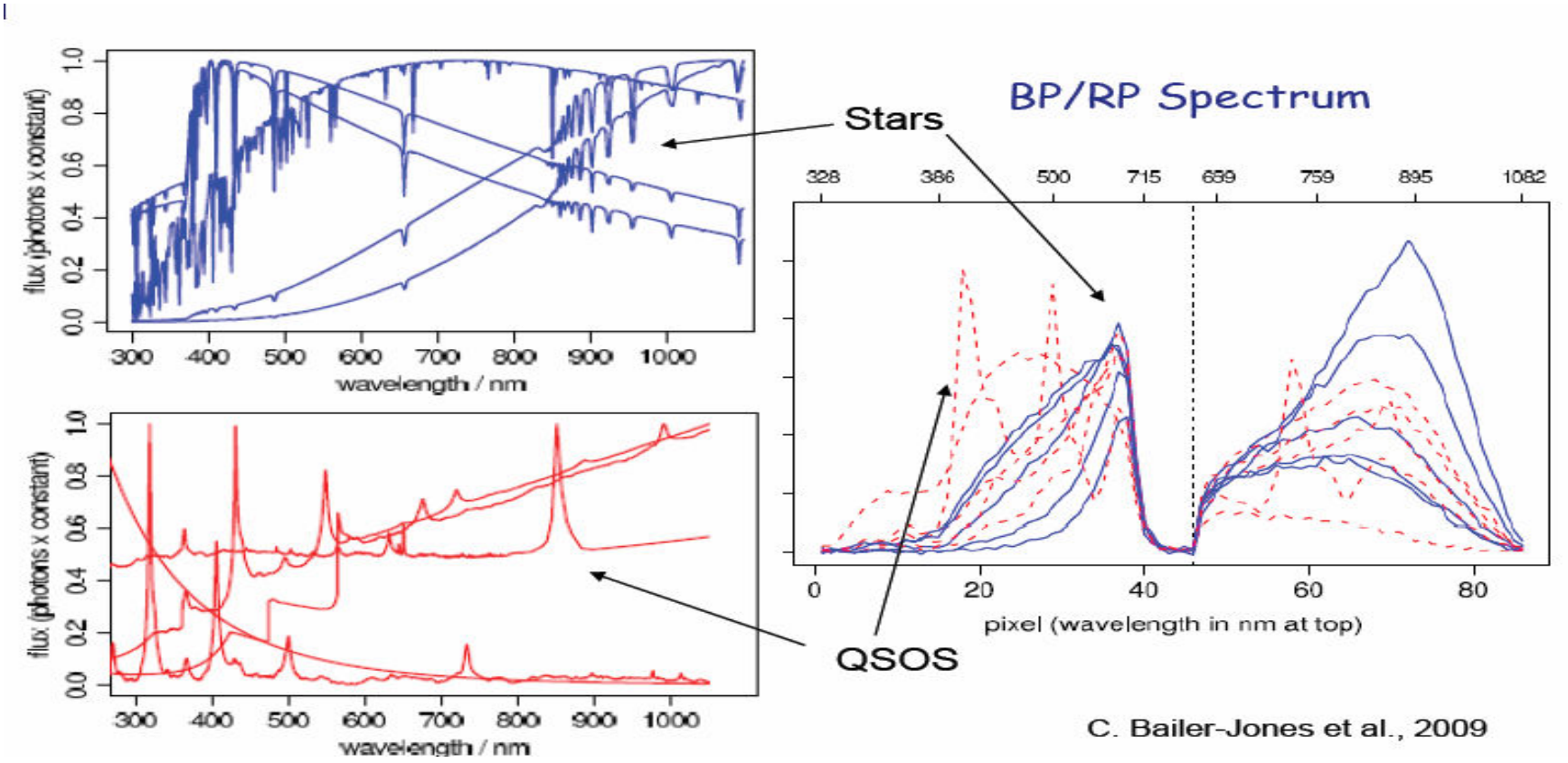

Purpose of the GIQC - The GIQC_5 in the MDB

What it is

♦ It is a compilation of QSOs from the literature. And in the literature under QSO are included active galactic nuclei objects (AGN) at large, that is radio loud quasars, Blazars, radio quiet quasars, BL LACs, Seyfert galaxies, LINERS. Thus, in the GIQC a QSO is an object which can be seen as an extragalactic quasi stellar source from a certain point of view and a given set of parameters.

♦ It aims to completeness. Objects were excluded if the redshift was unknown (except for quasars) or unreliable; or if the magnitude was quoted brighter than 10; or if the astrometric accuracy was worse than 1 arcsec.

♦ The precisions on position and on magnitude are modest, just to suffice to unmistakable match to the actual Gaia observation.

♦ The redshifts are useless for the main purpose of matching but are invaluable to feed the supervised Artificial Neural Networks (ANN) at the basis of the Gaia autonomous QSO detection.

♦ The morphology and variability indexes are merely indicative, in the statistical meaning, but this knowledge is required to understand and model the astrometric error budget, and to accept an object to form the core GCRF.

What it is not

♣ A Celestial Reference Frame

♣ The QSOs in the IGSL do form one, the LQRF

The GIQC_5 in a nutshell

Number of sources	1,248,372
Sources with magnitude	1,246,512
Sources with redshift	1,157,285
Astrometry precision	1 arcsec
Magnitude precision	0.5
Redshift precision	0.01
Average density	30.3 sources/deg^2
Average neighbor distance	3.7 arcmin (σ 4.9 arcmin)
Maximum distance to neighbor	5.2 deg
Maximum distance to neighbor (average of 100 larger values)	3.0 deg (σ 0.6 deg)

Sky density distribution

10 deg cells
log10 counts
equatorial

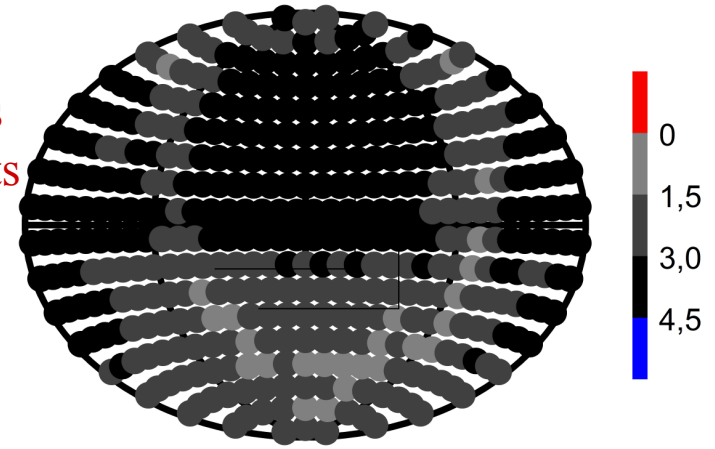

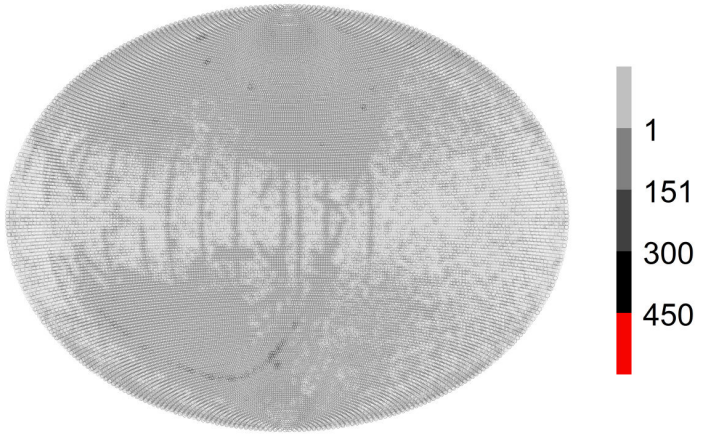

1 deg cells, linear counts, galactic

How the GIQC is formed

♦ Start from the LQAC2 list (Souchay et al., 2012), that contains 187,504 quasars. Accept the SDSS (Schneider et al, 2010, and references there in) originated objects, amounting to 116,105 quasars. Accept the 2dF/2qZ (Croom et al, 2004) originated objects, amounting to 22,835 quasars. Accept the BOSS selection (Paris et al, 2012, and references there in) originated objects, amounting to 87,822 quasars.

♥ Accept the ICRF2 (Fey et al., 2010), VLBA-6th supp calibrator list (Petrov et al., 2008), and VLA-2009 update calibrator list (NRAO, 2012), plus the list of candidates for the future reconciliation between the GCRF and the ICRF (Bourda et al., 2010), amounting to 4,925 objects, after removing the redundant entries. Redshift and optical magnitudes were searched in various catalogs and in the available literature, in special searching for matches in the GSC2.3 (Lasker et al., 2008) and USNO B1.0 (Monet et al., 2003). Still, 894 objects lack magnitude and 2,204 lack redshift. Likewise, 694 objects have extended morphology. Notwithstanding all the radio-selected quasars are included because of their key role to redress the future GCRF towards the ICRF, as well as to fill gridpoints near the galactic plane (1,539 objects) - and, again, once actually spotted by Gaia, to enrich the ANN templates.

♣ Consider the SDSS photometrically selected quasar candidates (Richards et al, 2009; Bovy et al, 2011), amounting to 887,406 objects. For the remaining quasars in the LQAC2, and further, which come from smaller catalogues, the analysis was made catalog by catalog, up to case by case.

GIQC Magnitude and Redshift distributions – And what resulted

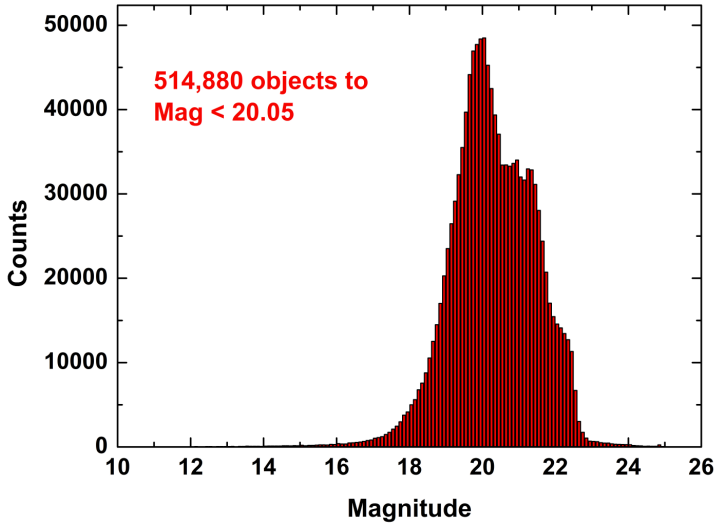

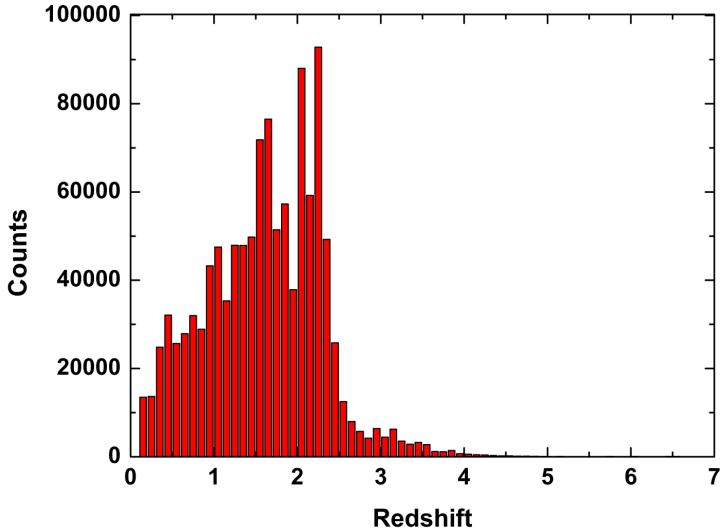

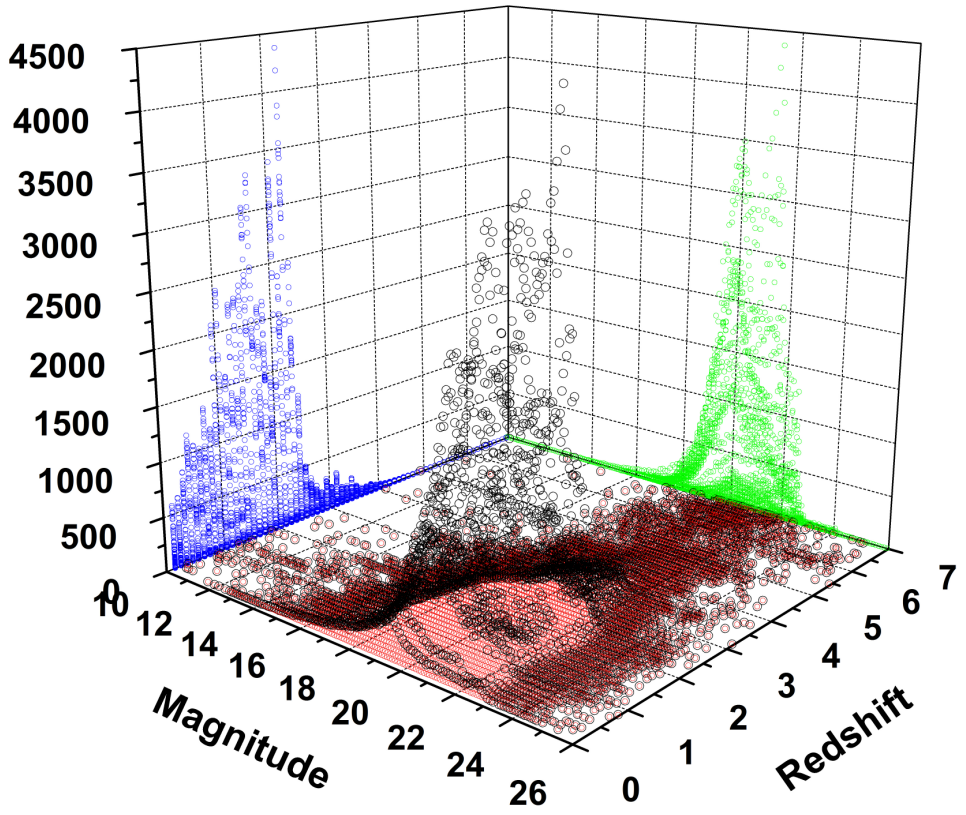

GIQC Classifiers

One-letter classifications in a nutshell

Flag	Column	Quantity	Description
D	1	191,802	Defining - spectroscopic redshift
C	1	52,954	Candidates - reliable but only photometric redshift
O	1	1,003,616	Other - either magnitude and/or redshift issues
S	2	208,298	SDSS lists belonging
V	2	4,866	VLBI (or long base interferometry) position
L	2	599	Link candidate source, optimal magnitude and radio position
A	2	14,527	AGN, pointlike or core dominated
B	2	512	Bulge dominated extragalactic source
R	2	38,699	Radio position available, although of lower precision
P	2	1,026	Poor observational history, otherwise no issues
U	2	960,173	Unreliable detection (for this catalogue purposes)
F	2	5,208	Faint source
E	2	957	Empty field in the optical domain
G	2	13,507	no remarkable characteristic

GIQC homogeneous sky distribution

Sky distribution of the main classifications

♦ From left to right the sky density distribution of the defining, candidate, and other sources in the GIQC_5. Each point in the plots represents equal area cells of radius 10 deg, on equatorial coordinates and logarithm scale.

♥ The defining sources are adequately represented over all sky, eventhough the SDSS area is clearly the most populated whereas the galactic plane even presents 3 empty bins.

♠ Further densification of the defining sources would only arise by the certification of new sources (using Gaia own means) or those presently classified as candidate or other. Special programs are being developed by this WP to determine magnitude and morphology of VLBI sources. And to densify the galactic plane content, mostly in association to LAMOST groups.

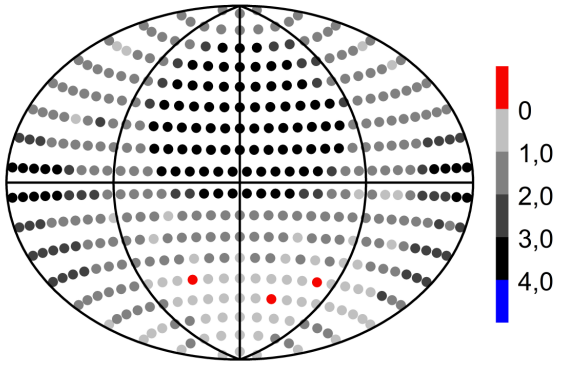

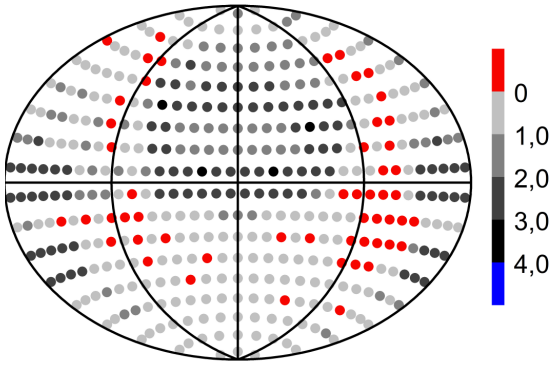

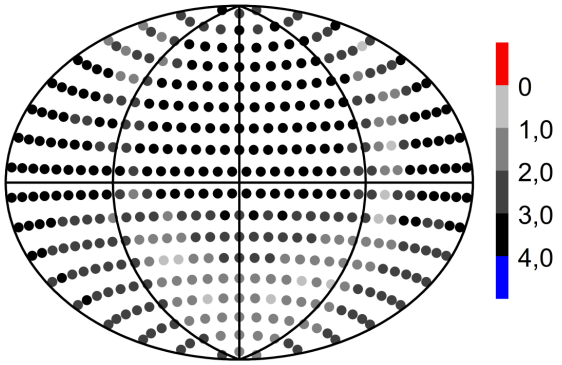

GIQC Morphological Indexes – Host galaxy review

- ♠ The host galaxy luminosity seems to increase proportionally to the strength of the central source, i.e. QSOs host galaxies may expected to usually be brighter than those around less powerful AGNs. Its absolute magnitude should be brighter than -23.5.
- ♠ The size of the host galaxy also tends to follow the rule. Typical sizes for BLLac are 13kpc. Most of times it is an elliptical or bulge dominated galaxy.
- ♠ Host galaxies have regularly been resolved for AGNs to z < 1.5 and 1arcsec resolution.
- ♠ The QSO space distribution peaks at z=0.6 for B=19, and at z=1 for for B=20.
- ♠ The largest fraction of GAIA QSOs will be of nearby ones. Average z = 1.1 but z = 0.8 at MAGr ~<18

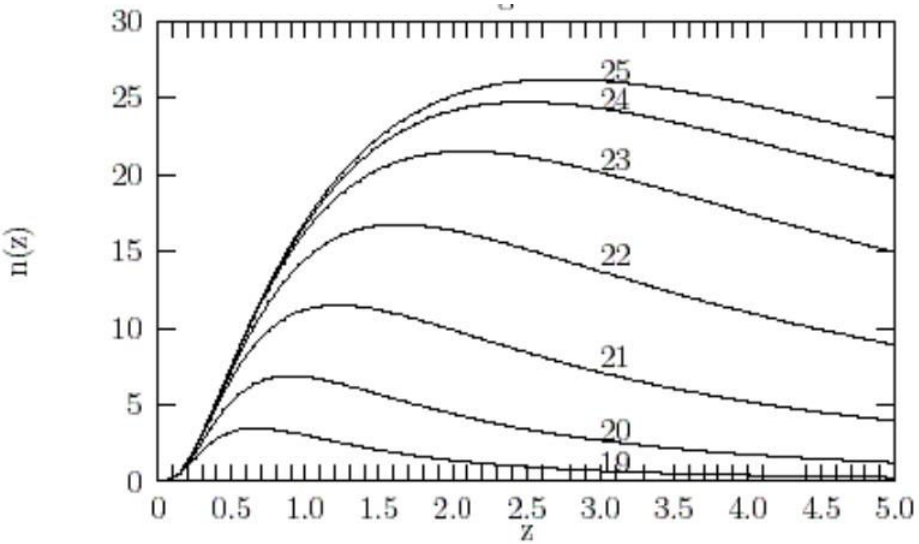

Number of quasars per deg^2 as function of redshift and magnitude (Crawford 1994)

GIQC Morphological Indexes – Host galaxy isophotes

SDSS DR9 image **GALFIT model** **residuals**

Model	x_c	y_c	m	r_e	n	b/a	θ_{PA}
psf	51.33 ± 0.00	51.19 ± 0.00	16.57 ± 0.00	–	–	–	–

GALFIT output

Residuals have significance 2.61 % (global) — 3.29 % (local)

1D visualization [Ellipse/IRAF/STSDAS]

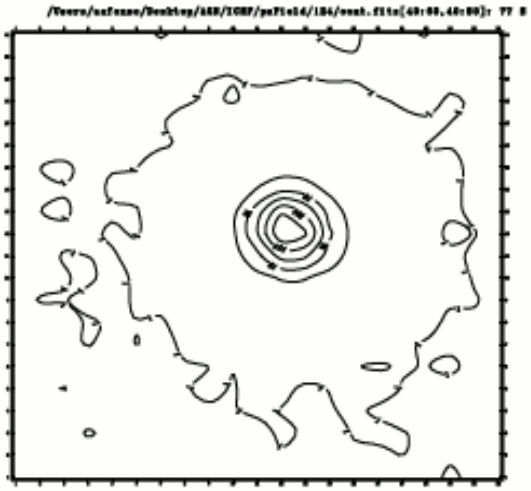

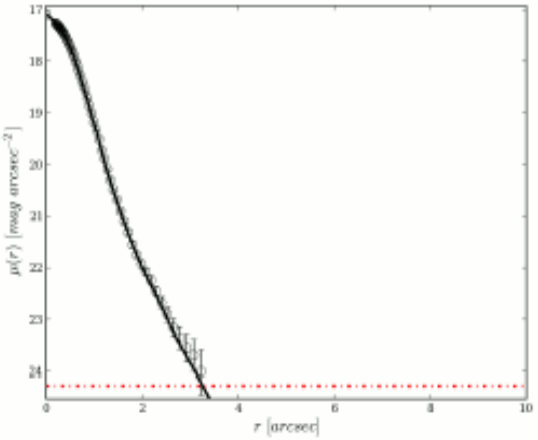

GIQC Morphological Indexes – Host galaxy isophotes

SDSS DR9 image **GALFIT model** **residuals**

Model	x_c	y_c	m	r_e	n	b/a	θ_{PA}
psf	51.14 ± 0.00	51.25 ± 0.00	15.58 ± 0.00	–	–	–	–
sersic	51.02 ± 0.02	51.45 ± 0.02	16.55 ± 0.01	9.26 ± 0.14	1.99 ± 0.04	0.72 ± 0.01	31.98 ± 0.81

GALFIT output

Residuals have significance 1.10 % (global) — 0.99 % (local)

1D visualization [Ellipse/IRAF/STSDAS]

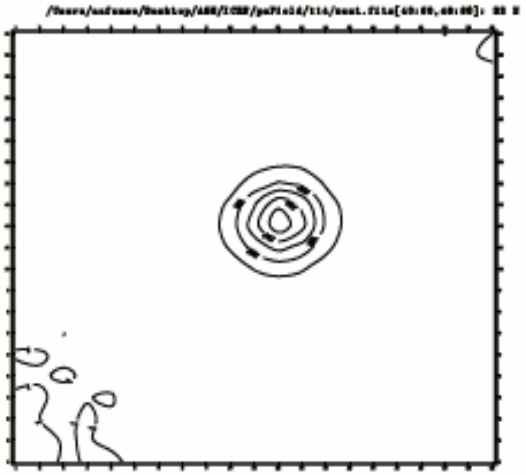

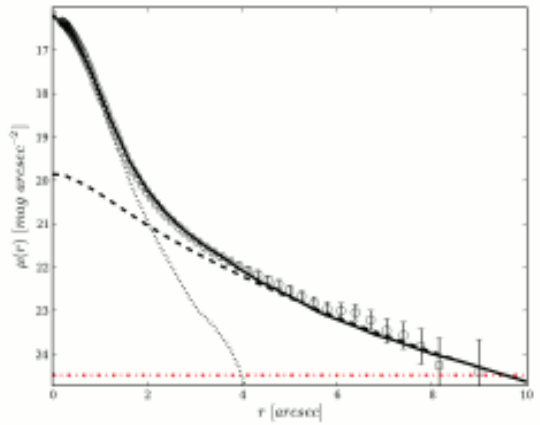

GIQC Morphological Indexes – GIBIS detection

V=12

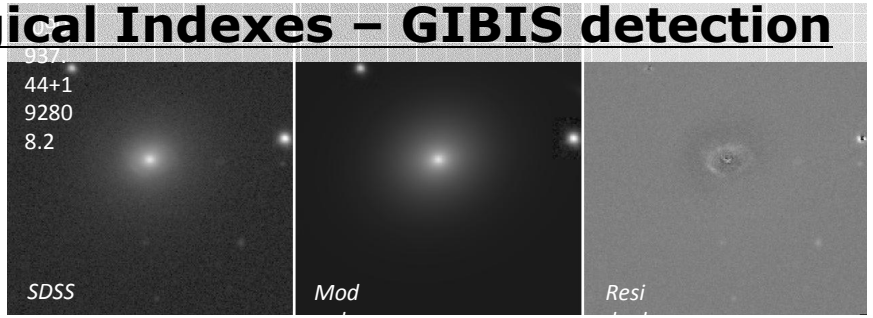

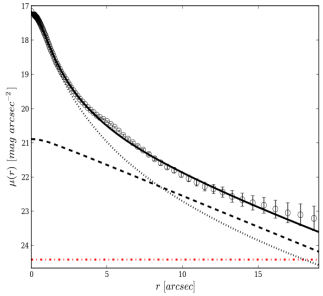

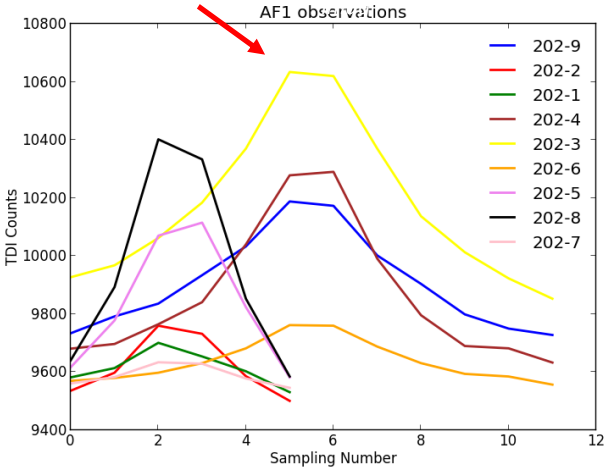

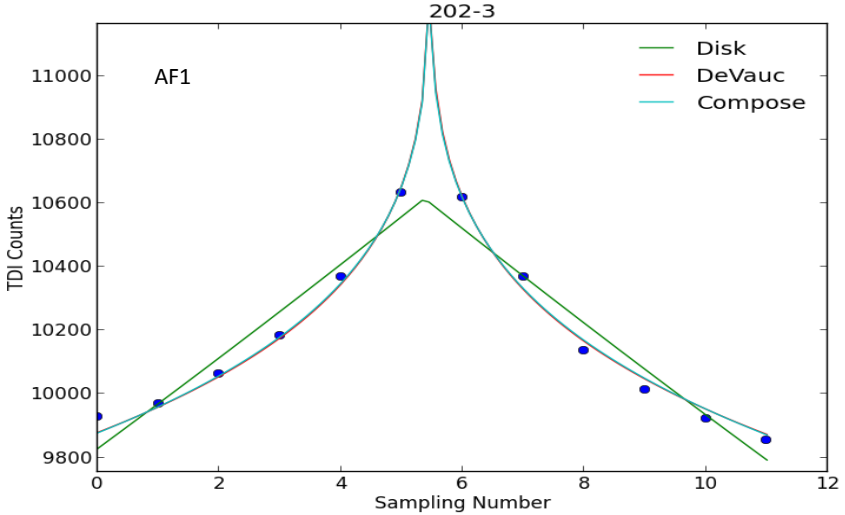

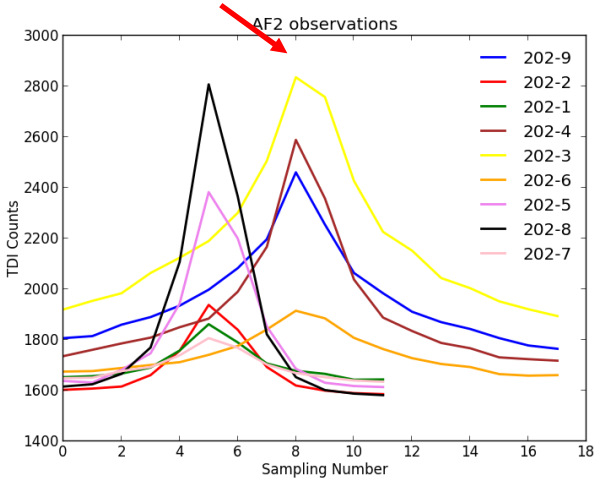

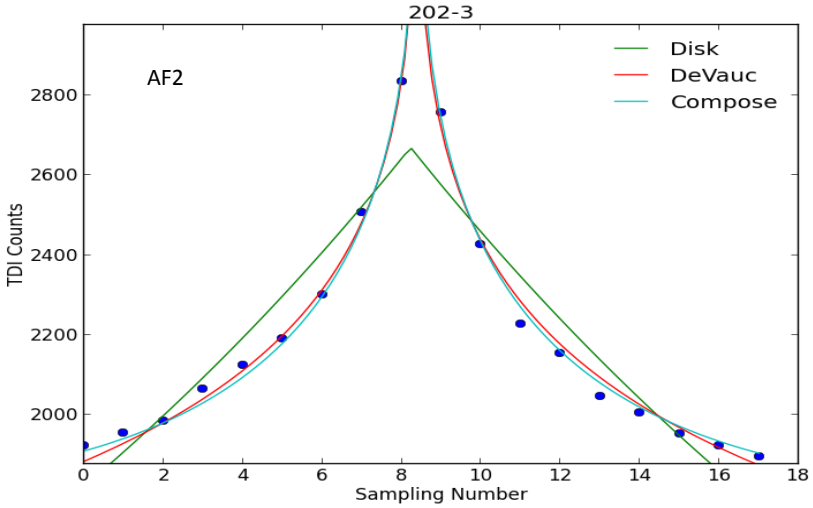

GIQC Morphological Indexes – Review

Model

♦ $I_{PC}(Q) = |P_Q - \overline{P_s}| / \sigma_s$

where I is the morphological index of quasar Q for the PSF parameter P in the color C, given in comparison to the mean value from the stars s, and normalized by the stellar standard deviation σ. Parameters are IRAF's sharp, Sround, and Ground.

♥ 1,343 objects covering the SDSS spaces.

Correlation to the SDSS class = 0.86

Object	Morphological Indexes - Rate of non-pointlike objects					
	SHARP field	SROUND field	GROUND field	SHARP class	SROUND class	GROUND class
QSO(DR7) $_{IP>2}$	0.19	0.31	0.43	0.55	0.23	0.33
QSO(DSS2) $_{IP>2}$	0.13	0.39	0.41	0.27	0.32	0.36
STARall	0.01			0.01		
STAR$_{\Delta M=1}$	0.01			0.01		
QSO(DR7)$_{IP>3}$	0.06	0.17	0.20	0.40	0.11	0.17
QSO(DSS2) $_{IP>3}$	0.04	0.21	0.24	0.11	0.15	0.20

♠ The rate of "extended quasars" increases towards lower frequencies, showing the astrophysical and cosmological signature.

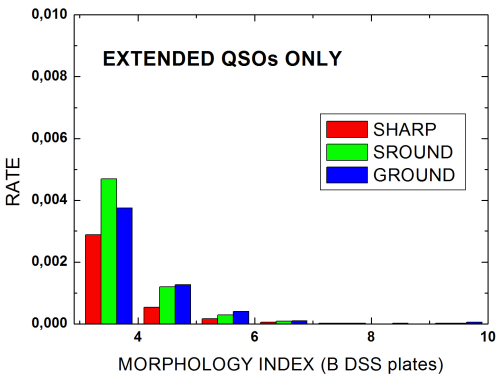

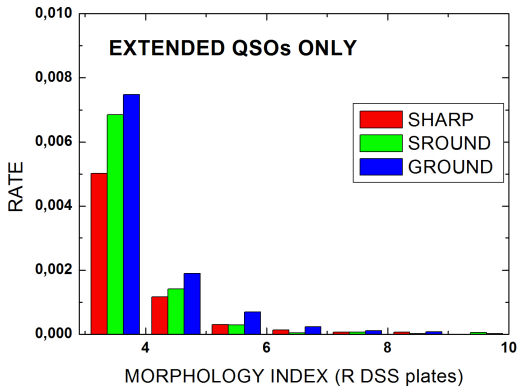

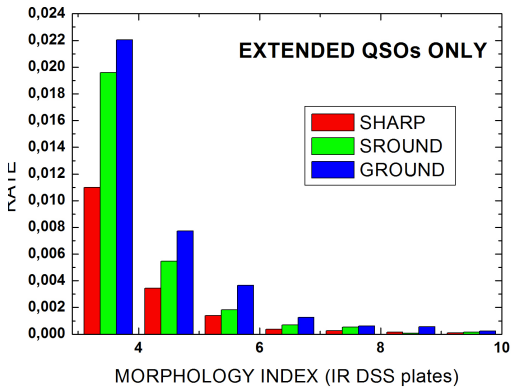

GIQC Morphological Indexes – Action Items

♥ In the earlier version GIQC_4 most sources had full morphological indexes (78% of the catalog, and 88% of the defining sources). Since 1,060,867 sources have now been added in the GIQC_5, the search of their images in the DSS is to be done, still 56% of the defining sources already have full morphological indexes.

♣ Presently, for the new objects the available indexes of stellar appearance was adopted, keeping their YES/NO natures by assigning respectively the values 1.00 or 3.00 under the R Ground column. As that, 99.6% of the catalog has at least one morphological index.

♠ Observational programs are being conducted by this WP at the ESO2.2, NOT, and CASLEO telescopes, to determine B and R magnitudes and morphology for the QSOs that will employed for the future orientation of the GCRF axis along the ICRFn.

♦ Morphological study of the defining ICRF2 sources present in SDSS images, by.Sonia Anton and Ana Afonso (MSc) as shown in the previous slides.

GIQC Variability Indexes – Scanning law monitoring

♦ The preceding and following astrometric fields of view (i.e., separated by an angle of 106 deg) have a repetition observing pattern of: 1h46m-4h14m-1h46m-4h14m.

♦ Typically, the objects are observed during 4-5 orbits and then gaps of about 30-40 days will separate these grouped measurements (depending of the object position).

♦ When an object is temporarily at the node of the great circle of scanning, it is regularly observed for several days.

♦ Thus Gaia has excellent capabilities to derive QSO variability. Such a record will have an enormous impact for QSO astrophysics.

♥ But, before that, it can enable to recognize QSOs, and to enlarge the supervised the ANN at the basis of the Gaia autonomous QSO detection.

♥ On the other hand, in the cases in which the photometric variability relates to the photocenter jitter, it can alleviate the QSO's error budget –
and exactly for the closer and brighter.

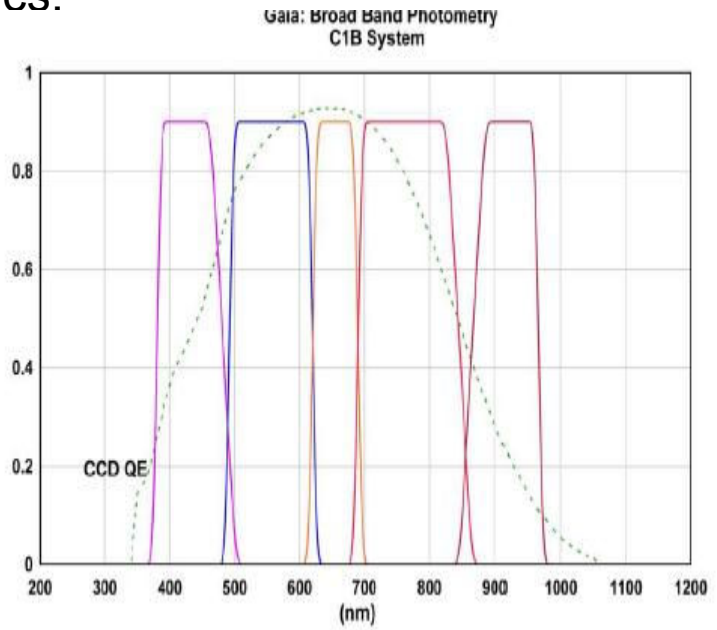

GIQC Variability Indexes – Rational

♣ **Popovic et al. (2011) model** – Associated astrometric and photometric variability due to

♠ Instabilities in the accretion disk

M_{BH} ($M_\odot$)	z				
	0.01	0.05	0.10	0.15	0.20
10^8	0.036	0.007	0.004	0.003	0.002
10^9	0.355	0.074	0.039	0.028	0.022
10^{10}	3.550	0.744	0.394	0.278	0.220

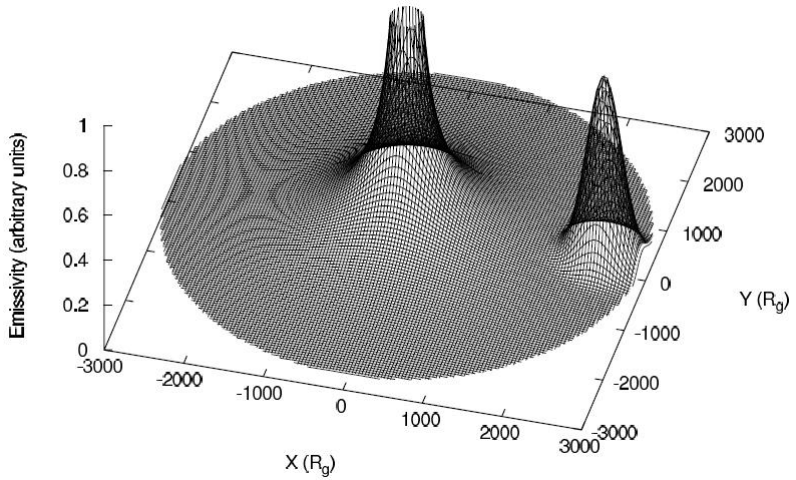

♥ density irregularities in the dusty torus

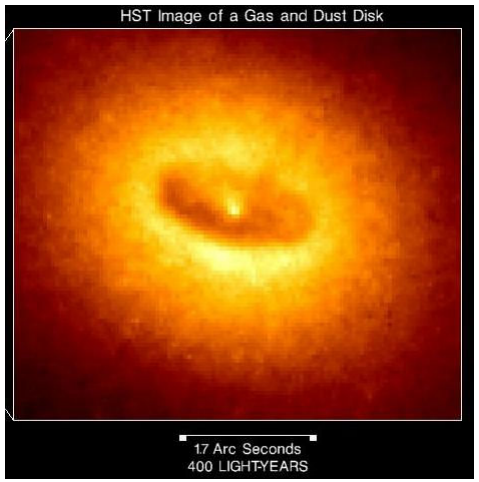

L ($10^{11} L_\odot$)	z		
	0.01	0.05	0.10
0.50 μm			
3	1.579	0.208	0.039
6	8.400	1.886	0.860
10	8.170	1.353	0.693

GIQC Variability Indexes – Model

♣ from z and V calculate Mabs (absolute magnitude) (Souchay et al, 2009)

♣ from Mabs calculate the QSO mass Mbh and luminosity (Morgan et al., 2011)

♥ the accretion disk radius is calculated from the black hole mass by the rest-frame equation; or independently by ”absolute mag-log(radius)” adjustment of Shen et al (2008)

♥ from the accretion disk in cm, in the rest frame, its apparent angular radius in micro-arseconds is calculated using the redshift to derive the properangular size and it is adopted as the accretion disk variability index.

♠ the size of the disk torus is obtained from the inner radius scaled up by the expression of Barvainis (1987), which is consistent with Sluse et al. (2013).

♠ the disk torus apparent angular size in arc-seconds is calculated using the redshift, and is taken as the torus variability index.

♦ The variability indexes indicate that the larger the regions are, the larger the probability of happening an instability there.

♦ There are 89,129 disk radii found larger than 1 μ as. And 1,126,210 torus radii found larger than 100 μ as. Remembering also that the base of the jets, where there is optical emission, is commensurable to the torus size.

GIQC Variability Indexes – Action Items

♣ ESO Max Planck 2.2m telescope, La Silla, Chile, 0".238/pixel, WFI nearby the optical axis. Filters Rc/162 (peak 651.7nm, FWHM 162.2nm) and BB#B/123 (peak 451.1nm, FWHM 135.5nm). In each filter 3 frames are taken, to a combined SNR of 1000 (up to 2h total integration time).

♣ Relative astrometry (1mas) and photometry (0.001mag)

$$C_n^m - \langle C \rangle_n = C_0 + \sum_{i,j,k}^{1,3} A_{ijk}^m X^i Y^j M^k$$

♣ Linear Pearson correlation and Non-parametric Spearman correlation (statistical error in brackets).

QSO	ΔX /ΔMag		ΔY /ΔMag		JitterX/ ΔMag		JitterY/ ΔMag	
	Pearson	Spearman	Pearson	Spearman	Pearson	Spearman	Pearson	Spearman
1512-0905	-0.42 (0.59)	-0.49 (0.33)	0.85 (0.00)	0.77 (0.33)	-0.80 (0.43)	-0.94 (0.00)	0.79 (0.00)	0.89 (0.02)
1620+1724	0.94 (0.00)	0.90 (0.04)	0.81 (0.01)	0.80 (0.10)	0.31 (0.48)	0.00 (1.00)	-0.30 (0.71)	-0.60 (0.28)
1620+1736	0.14 (0.76)	0.03 (0.96)	-0.52 (0.53)	0.09 (0.87)	0.38 (0.29)	0.31 (0.54)	-0.75 (0.44)	-0.49 (0.33)
1751+0939	0.58 (0.41)	0.50 (0.67)	-0.83 (0.73)	-0.50 (0.67)	0.96 (0.02)	1.00 (0.00)	0.62 (0.35)	0.50 (0.67)
0522-6107	0.44 (0.14)	0.46 (0.29)	-0.31 (0.62)	-0.32 (0.48)	0.22 (0.55)	0.36 (0.43)	0.15 (0.70)	0.14 (0.76)
0407-1211	-0.03 (0.97)	0.00 (1.00)	-0.12 (0.89)	-0.41 (0.60)	0.64 (0.13)	0.40 (0.60)	0.66 (0.11)	0.80 (0.20)
0442-0017	-0.46 (0.70)	-0.41 (0.60)	-0.40 (0.73)	-0.40 (0.60)	0.04 (0.96)	-0.80 (0.20)	0.40 (0.45)	0.40 (0.60)
0858+1651	-0.74 (0.61)	-0.20 (0.80)	-0.10 (0.91)	-0.20 (0.80)	-0.73 (0.61)	-0.20 (0.80)	-0.57 (0.66)	-0.80 (0.20)
1218+0200	0.03 (0.97)	0.20 (0.75)	-0.42 (0.64)	-0.50 (0.39)	-0.52 (0.59)	-0.70 (0.19)	-0.41 (0.65)	-0.30 (0.62)

Teerkopi (2003) QSOs selected for high amplitude, long term variability. This time-line 2.25y, at every 2-3 months, i.e. 5-8 runs/source.

GIQC Variability Indexes – Action Items

♣ 41 QSOs of the Deep 2 field were analyzed. QSOs images obtained during 4.5 years with the Canada France Hawaii Telescope (CFHT) in the frame of the CFHTLegacy Survey (CFHT-LS). All quasars showed variability, but the evidence of correlation is weak due the use of absolute astrometry.
♣ Relative PSF astrometry and photometry in the case of a QSO with a nearby star, evidentiates the correlation.

♣ CFHT image of the QSO 39436 with the nearby star (5” south). Correlation between the photocenter walk (green line) and the Blue and red magnitudes variation.

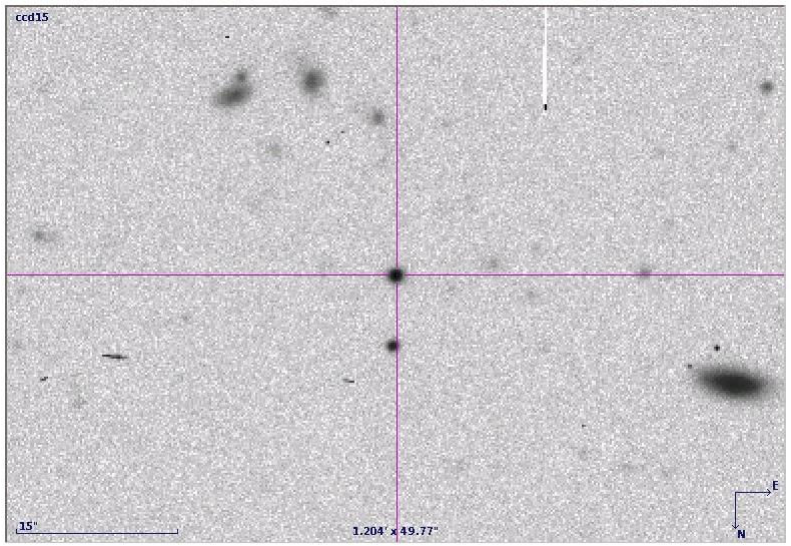

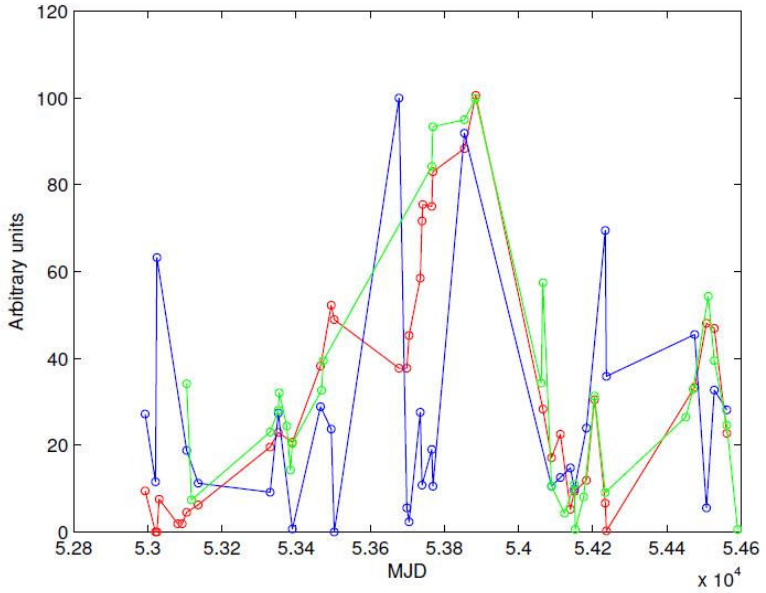

GIQC Variability Indexes – Action Items

♣ Variability modulus based on Kelly et al. (2009):
V= A (Δ t/y) $^{\gamma}$

♦ Zadko Telescope Variability program

(Taris et al.)

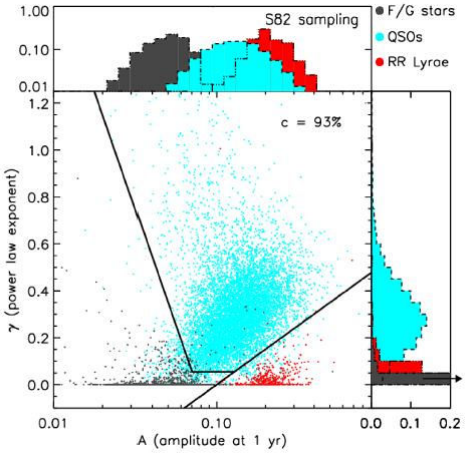

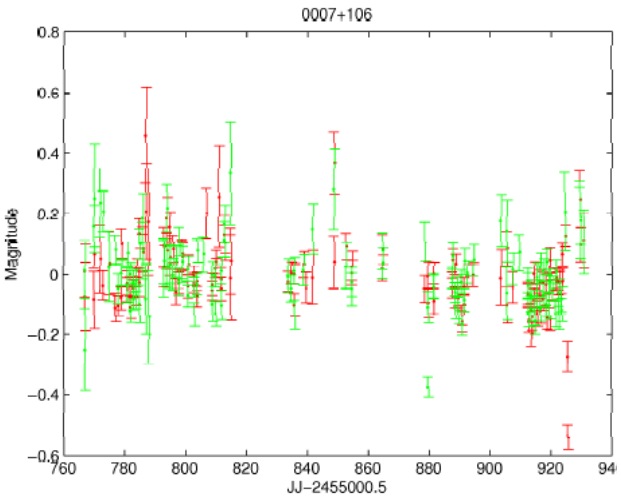

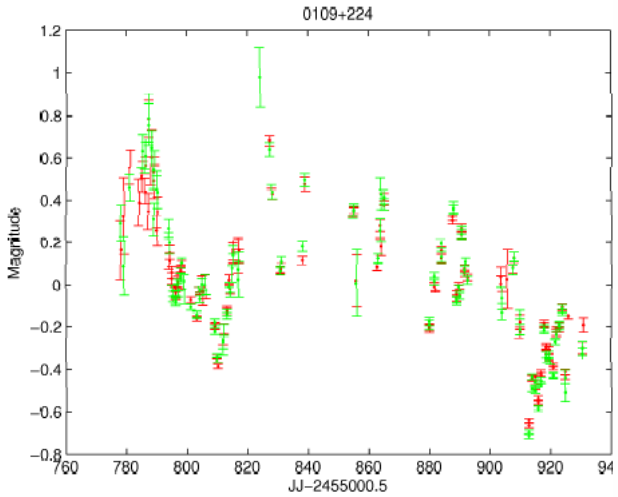

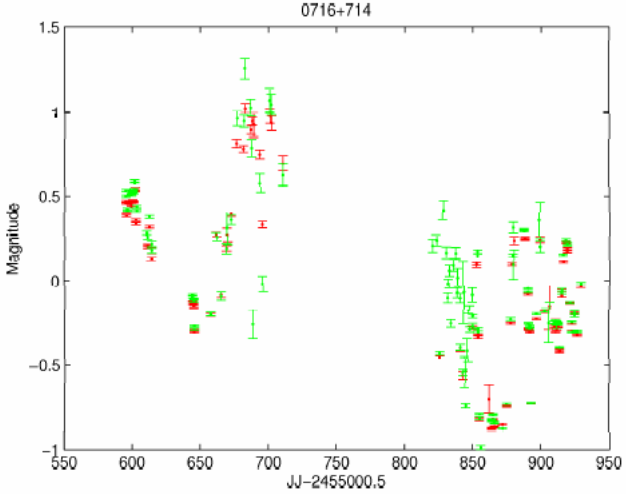

A = 0.348 ±0.006

γ = 0.484 ±0.0009

A = 0.394 ±0.003

γ = 0.558 ±0.0003

A = 0.390 ±0.003

γ = 0.613 ±0.0005

THE GAIA INITIAL QSO CATALOGUE – GIQC_5 IN THE MDB

RA (deg)	DEC (deg)	MAG	z	Bshr	Bsrn	Bgrn	Rshr	Rsrn	Rgrn	Ishr	Isrn	Igrn	Vdisk	Vtorus	Class
0.001997	-0.451102	20.50	0.250						3.00				0.03	0.14	D S
0.005750	-30.607472	19.50	1.143				0.20	0.01	0.91				0.34	0.57	D
0.007333	-31.373833	19.86	1.331				0.73	0.44	0.00	1.82	1.14	1.37	0.32	0.55	D
0.008067	-0.240971	19.93	2.163						1.00				0.57	0.83	D S
0.013229	1.252967	20.74	2.354						1.00				0.41	0.69	D S
0.022875	-27.419556	19.14	1.930				0.12	1.01	0.41				0.88	1.08	D
0.027231	0.515332	20.49	1.823				0.73	0.48	0.26	0.63	1.07	0.20	0.30	0.54	D S
0.031618	0.495354	20.38	2.254						1.00				0.49	0.77	D S
0.033300	-63.593300	17.00	0.136				0.42	0.95	0.17				0.22	0.59	D S
0.033946	0.276292	20.02	1.839				1.18	1.10	0.49	0.71	1.07	1.09	0.43	0.68	D S
0.038609	15.298489	19.38	1.204	0.36	0.92	0.08	0.92	0.02	0.30	1.11	1.51	1.46	0.39	0.63	D S
0.038657	2.106112	19.46	1.432						1.00				0.48	0.71	D S
0.039099	13.938458	18.43	2.225	0.63	0.91	0.09	0.59	0.23	0.14	2.07	0.16	1.43	1.79	1.71	D S
0.039264	-10.464410	18.97	1.854						3.00				0.94	1.12	D S
0.040375	-31.279972	18.65	1.727				1.16	1.47	0.77	1.11	2.66	3.78	1.06	1.19	D
0.041250	-30.924944	18.37	1.787				0.39	0.07	0.03				1.37	1.41	D
0.047551	14.929367	19.36	0.460	0.07	0.09	0.02	0.18	0.76	0.04	0.17	1.33	0.59	0.12	0.31	D S
0.048197	-8.835659	19.06	3.220										3.65	2.84	D S
0.048583	-31.644417	19.38	2.680				0.95	0.43	1.43				1.60	1.64	D
0.049839	0.040359	17.85	0.480				0.42	1.11	0.44	0.36	1.16	0.18	0.37	0.63	D S
0.051083	-0.539051	20.33	1.436				0.99	0.27	0.38	0.01	0.41	0.29	0.25	0.48	D S
0.054310	4.734323	20.89	2.624						1.00				0.47	0.76	D S
0.054787	14.176304	19.12	0.949	0.86	1.20	0.30	0.36	0.96	0.48	0.40	1.99	1.41	0.36	0.59	D S

THE GAIA INITIAL QSO CATALOGUE – NOTE ADDED IN PROOF

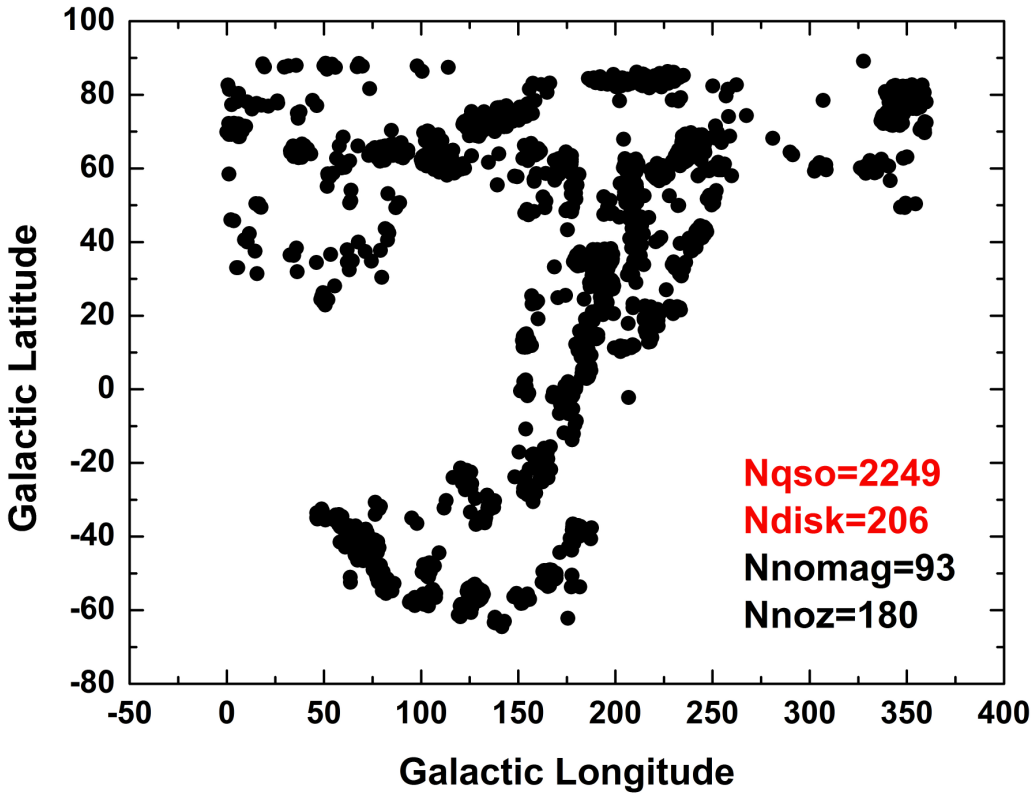

☻ First delivery of LAMOST QSOs. SDSS area.

♥ 5017 QSOs.

♠ 2430 QSOs not found by SDSS photometric criteria.

♦ 2249 QSOs matching the GIQC criteria of magnitude and redshift.

♣ 206 objects in $|b| < 20$deg

☺ Spectroscopy of other 359 galactic plane QSOs are scheduled for the current period

Large Sky Area Multi-Object Fibre Spectroscopic Telescope (LAMOST), meridian reflecting Schmidt telescope, located in Xingiong Station, Hebel Province, China.
 # two rectangular mirrors, made by 1.1m hexagonal deformable segments, focal plane of diameter 1.75m ≈ 5deg field of view. Nominal limit at 20.5mag.
 # 4000 fibres at precision of 3arcsec, with 'blue' (370-590nm) and 'red' (570-900nm) detection. Also operates on high spectral resolution mode in the range 510-540 and 830-890nm.

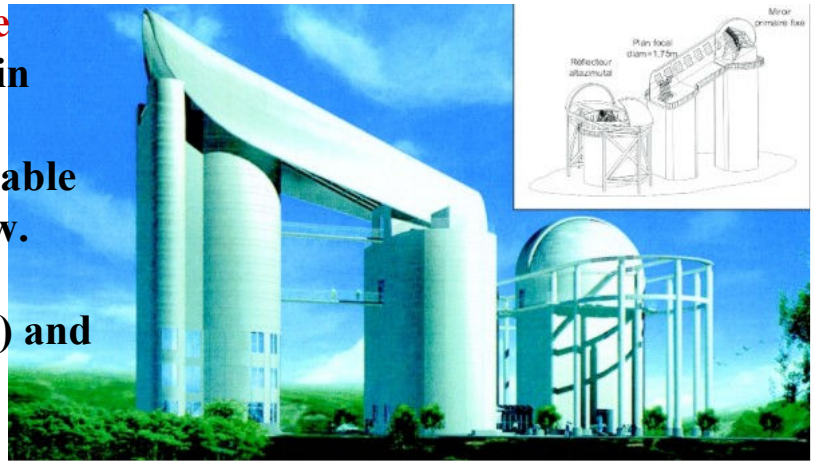

Gaia 65 days to launch and counting


Just steady with that L2 point now
LE VOYAGE DANS LA LUNE. EN PLEIN DANS L'ŒIL !! (9e TABLEAU)